

# Toward Label-Free Optical Multiplexing of Analytes in Indicator Release Lateral Flow Assays via Detection Zones Containing Tailored Capture Materials

Estela Climent,<sup>[a]</sup> Wei Wan,<sup>[a, b]</sup> and Knut Rurack\*<sup>[a]</sup>

The use of macromolecules and materials immobilized in the detection zone of test strips for indicator capture and focusing in label-free lateral flow assays (LFAs) is described, with emphasis on its future use in low number multiplexing. Several materials such as polyelectrolytes, functionalized mesoporous silica micro- and nanoparticles, chemically modified cellulose or glass fibre (GF) membranes and molecularly imprinted polymer gels coated onto membranes were studied in model assays, before the most promising materials were combined with antibody-gated indicator delivering (gAID) sensor materials.

Cellulose, nitrocellulose and GF membranes were used as supports and highly fluorescent dyes of different charge states as model indicators. Combination of the best performing capture materials with gAID systems made it possible to distinctly increase the sensitivity and reduce the measurement uncertainty in the LFA testing of pentaerythritol tetranitrate (PETN) in aqueous samples. In addition, dual-plexing of PETN and 2,4,6-trinitrotoluene (TNT) was realized on a single test strip containing two dedicated capture zones.

## Introduction


Methods for the rapid and sensitive detection of key analytes outside of a dedicated laboratory infrastructure are increasingly gaining importance in medical diagnostics and environmental monitoring, in the security, occupational health and safety as well as food sectors.<sup>[1]</sup> They have moved into the focus of societal attention decisively within the last 2 years because of the development of rapid tests to help contain the SARS-CoV-2 pandemic.<sup>[2]</sup> Among the rapid testing methods employed, lateral flow assays (LFAs) are perhaps the most commonly used because of their ease in handling for nontrained people and many test kits based on the technique are available on the market.<sup>[3]</sup> This type of assay usually comprises a membrane strip, such as cellulose, nitrocellulose or glass fibre, in which a cocktail comprising the ingredients of the sample and, depending on the type of assay, a binder, a labelled binder, a label carrying various binders or an indicator is transported to the detection area through the capillary forces that flow the liquid within the fibrous membrane.<sup>[4]</sup> The membrane is basically divided into a sample application zone and a detection zone, in


which commonly a capturing reagent or binder, often an antibody, is immobilized. Upon advent of the LFA cocktail, a characteristic pattern of coloured lines is formed in the detection zone, giving a positive or negative test result. An absorbing pad at the end of the strip ensures a continuous capillary flow of the liquid. Currently, labelled bio(macro)molecules such as conjugated antibodies or immunoactive reagents<sup>[5]</sup> as well as aptamers<sup>[6]</sup> are primarily used as binders. However, for the adaption of LFAs for small molecule detection, several key issues need to be considered. A major drawback is that most of the capture agents either indicate the analyte only indirectly, through competition with a labelled analogue, or follow the traditional indicator approach that has to accomplish selective and sensitive binding as well as generating an intense signal, which is often difficult to achieve and, in many cases, reduces sensitivity considerably. Another limitation of such capture agents is that only a few analytes can be measured per assay,<sup>[7]</sup> and often a second binder (e.g., a labelled secondary antibody) is required for indication.

An alternative strategy to lateral flow assays for small-molecule detection is gated indicator release. Such assays rely on highly porous nano- or microparticles that are loaded with indicator molecules, the pores being closed by a dedicated gatekeeping or capping chemistry (Figure 1A, Scheme S1 for details on chemical structures).<sup>[8]</sup> These caps, often also antibodies or aptamers as in antibody/aptamer-gated indicator delivery (gAID) systems,<sup>[9]</sup> interact with a hapten derivative (the so-called "gatekeeper"), an analogue of the target analyte that is grafted to the outer particle surface, and ensure that the indicator is not released in the absence of an analyte. When analyte molecules are present in a sample, they can bind to the biomacromolecule thus leading to a dissociation of the gatekeeping complex and entailing the unhindered diffusion of the stored indicator molecules out of the pores (Figure 1A). Both,

[a] Dr. E. Climent, Dr. W. Wan, Dr. K. Rurack  
Chemical and Optical Sensing Division  
Bundesanstalt für Materialforschung und -prüfung (BAM)  
Richard-Willstätter-Str. 11, D-12489 Berlin, Germany  
E-mail: knut.rurack@bam.de

[b] Dr. W. Wan  
Surflay Nanotec GmbH  
Max-Planck-Str. 3, D-12489 Berlin, Germany

 Supporting information for this article is available on the WWW under <https://doi.org/10.1002/anse.202100062>

 © 2022 The Authors. Analysis & Sensing published by Wiley-VCH GmbH. This is an open access article under the terms of the Creative Commons Attribution Non-Commercial License, which permits use, distribution and reproduction in any medium, provided the original work is properly cited and is not used for commercial purposes.

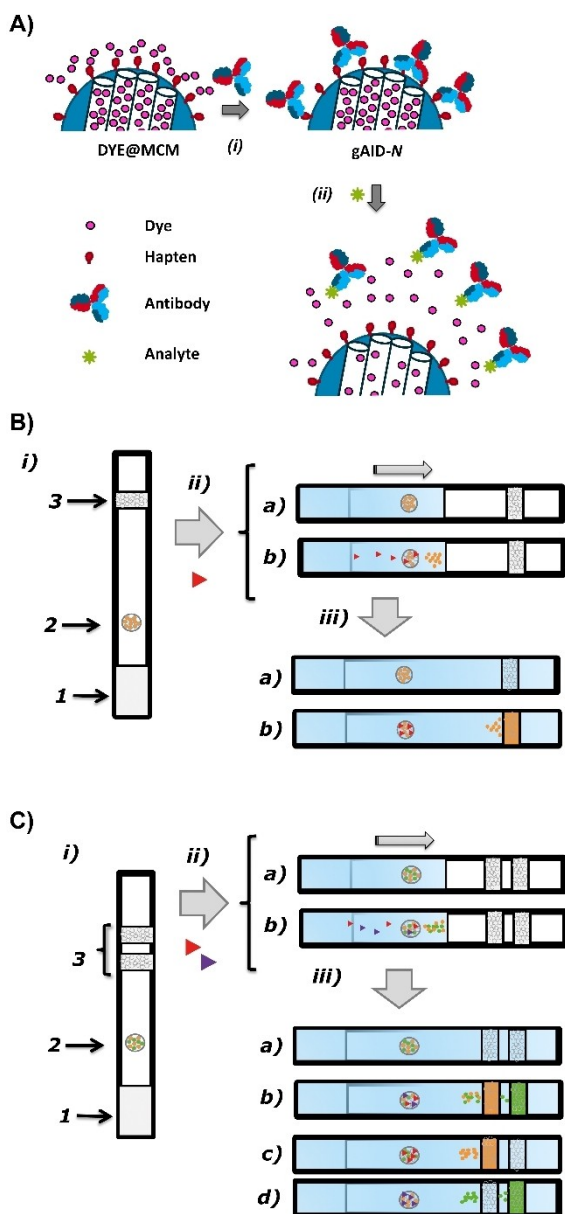


**Figure 1.** A) Basic principle of operation of gAID systems. Indicator dyes are loaded into the mesoporous host particle, haptens are attached to the outer surface and the pores are closed with antibodies (i). Advent of the analyte leads to an opening of the pores and release of the indicator (ii); see Scheme S1, Supporting Information for chemical details of the components. Working principle of a gAID LFA on strip for the detection of (B) a single analyte (red triangle) and (C) two analytes (red and violet triangles). i) Strip architecture with sample introduction zone (1), gAID material-containing interaction zone (2) and detection zone (3); ii) dipping of strip into a sample and start of development; iii) late stage of development. The example in (B) shows a test strip containing one focusing line (3) that can capture a specific indicator (orange dots) after release and flow: a) blank sample does not lead to release; b) a sample containing the analyte leads to release of orange dye. The example in (C) shows a test strip containing two different focusing lines (3) that can capture a specific indicator (orange and/or green dots) after release and flow: a) blank sample does not lead to release; b) a sample containing both analytes leads to release of both dyes; c) "red" analyte leads to release of orange dye; d) "violet" analyte leads to release of green dye.

the analyte-antibody complex as well as the indicator are transported with the flow, but in contrast to traditional LFAs, not the antibody needs to be detected, but the designated

indicator (Figure 1B,C).<sup>[9]</sup> Because a large number of indicator molecules can be released when a single analyte molecule binds to a biomolecular cap, such systems show intrinsic features of chemical signal amplification,<sup>[8,10]</sup> allowing for multiplexing,<sup>[11]</sup> for instance by using more than one gAID material loaded with differently coloured/fluorescent dyes on a single strip, as well as for very sensitive analysis,<sup>[12]</sup> thus addressing two important challenges in contemporary LFA research.<sup>[13]</sup>

Until today, gAID-type LFAs have been optimized with respect to the porous host material,<sup>[14]</sup> the loading and release behaviour of indicators<sup>[15]</sup> and the affinity tuning of the gatekeeping biochemistry.<sup>[16]</sup> No particular attention has been paid yet to improving assay performance by concentrating the released indicator molecules in a designated focusing zone. Özalp's group has recently reported on a gAID-type LFA in which the loaded materials are arranged in lines and the analytical response is assessed as a signal decrease in those lines as a consequence of indicator release.<sup>[17]</sup> While this approach is certainly appealing, it is an indirect detection scheme, not taking full advantage of measuring the released indicator in a focused area. In the present work, we thus explored the possibilities of creating dedicated capture zones directly on/in the strips for the improved detection of released indicators, relying on electrostatic attraction of ionic polymers and functionalized mesoporous silicas as well as the recognition abilities of molecularly imprinted polymers. Our work shows that the sensitivity of such LFAs can be improved by at least an order of magnitude through implementing such features via tailored capture materials.

## Results and Discussion

**Working principle of a gAID LFA on strips.** The principle of a single-analyte and a multiplexed gAID LFA is depicted in Figure 1B,C. The sample is introduced at the sample introduction zone (1) and flows toward the interaction zone (2) in which the gAID material(s) is (are) deposited and the analytical reaction takes place. While the gAID material remains in zone 2, the liberated indicator, most commonly a dye, travels with the solvent front eventually reaching the area at the end of the strip. So far, the signal in this detection area as such was analysed after photographing the strip. For first attempts toward multiplexing two approaches have been realized to segmentize this area. On one hand, several indicators of different charge state and chemical nature have been used, allowing for chromatographic separation.<sup>[11]</sup> On the other hand, a single indicator has been used but several channels for LFA development, i.e., one channel for one analyte.<sup>[11]</sup> While chromatographic separation has its well-known limitations of potential tailing or asymmetric spots or bands, the multi-channel approach makes the system more complicated and dilutes the sample in the sense that the sample is divided into the different individual channels.<sup>[18]</sup> Implementation of a dedicated detection zone (3) with a focusing element – a capture material – thus seemed to be important. Being modular

in design, this section can also contain more than one capture material, targeting the capture of different indicator dyes for multiplexing detection.

**Types and implementation of capture materials in model assays.** The challenge of localizing reporter molecules liberated from one or more sensory materials in the course of a single- or multiplexed LFA in particular zones on a few-centimetre long test strip, to facilitate read-out with a widely used device such as a smartphone or tablet, was addressed by investigating the application of macromolecules and nanomaterials in specific regions of a strip, as well as by chemically modifying strips or impregnating them with imprinted polymer coatings (Table 1). While most approaches aim to capture charged, highly water-soluble dyes mainly used in such assays by electrostatic interactions, we have also developed molecularly imprinted polymeric (MIP) gel coatings grafted from the functionalized fibres of paper strips into which specific reporter molecules have been imprinted as templates. The latter strategy was based on the consideration that polyelectrolytes and amino- and carboxylic acid-modified mesoporous materials and membranes cannot distinguish between different molecules with

the same overall charge state. In a first series of experiments, the general suitability of the different approaches was assessed by spotting various dye solutions onto the interaction zone of the strips (zone 2, Figure 1) and conducting model assays, not yet involving the hybrid gAID materials of a gated indicator release assay.

**Polyelectrolytes as capture matrix.** The architecturally simplest strategy is the application of a polyelectrolyte as capture material. To assess the viability of this approach, poly(diallyldimethylammonium chloride) or PDDAC, representing a polycation, was selected to capture sulforhodamine B (SRB), a strongly orange fluorescent, anionic dye frequently used as cargo in gAID systems. As is detailed in Section 5, Supporting Information, PDDAC solutions of two different concentrations were applied to create lines with thicknesses of ca. 5 mm in zone 3 (Figure 1B) and the capture efficiency was tested by developing the model SRB assays with Milli-Q water (H<sub>2</sub>O) or phosphate-buffered saline (PBS; 0.8 mM, pH 7.5). Table 1 collects the main results, illustrated by representative images shown in Figures S7 and S8, revealing that especially when using the application-relevant buffer as mobile phase is

**Table 1.** Overview of the capture zone approaches reported in this work and their basic performance features; for details, see sections 5–8, Supporting Information.

Material	Capture	Application	Zone size	Substrate <sup>[a]</sup>	Mobile phase	Dye	Retention efficiency	Short-term stability (5 min)	Long-term stability (1 h)
PDDAC (17%)	Electrostatic	Solution, deposited	5 mm	GF	water	SRB	high	yes	yes
PDDAC (17%)	Electrostatic	Solution, deposited	5 mm	GF	PBS	SRB	moderate	yes	no
PDDAC (35%)	Electrostatic	Solution, deposited	3 mm	GF	PBS	SRB	high <sup>[b]</sup>	yes <sup>[b]</sup>	no
PDDAC (35%)	Electrostatic	Solution, deposited	6 mm	GF	PBS	SRB	high <sup>[b]</sup>	yes <sup>[b]</sup>	yes <sup>[b]</sup>
APTES-MCM	Electrostatic	Suspension, deposited	3 mm	NC	PBS	FLU	high	yes	yes
APTES-SBA	Electrostatic	Suspension, deposited	3 mm	NC	PBS	FLU	moderate	yes	no
COOH-MCM	Electrostatic	Suspension, deposited	3 mm	NC	PBS	FLU	none	no	no
APTES-MCM	Electrostatic	Suspension, deposited	3 mm	GF	PBS	FLU	high	yes	yes
APTES-MCM	Electrostatic	Suspension, deposited	3 mm	GF	PBS	SRB	high	yes	yes
COOH-MCM	Electrostatic	Suspension, deposited	3 mm	GF	PBS	Rh6G	high	yes	yes
COOH-MCM	Electrostatic	Suspension, deposited	3 mm	GF	PBS	Rh101	high	yes	yes
APTES-C	Electrostatic	Substrate, coated	5 mm	Cellulose	PBS	FLU	high	yes	moderate
APTES-GF	Electrostatic	Substrate, coated	5 mm	GF	PBS	FLU	moderate	yes	low
COOH-GF	Electrostatic	Substrate, coated	5 mm	GF	PBS	FLU	none	no	no
FLUMIP-GF	imprinted	Substrate, coated	5 mm	GF	PBS	FLU	high	yes	yes
FLUMIP-GF	Imprinted	Substrate, coated	5 mm	GF	PBS	SRB	none	no <sup>[c]</sup>	no
SRBMIP-GF	Imprinted	Substrate, coated	5 mm	GF	PBS	SRB	high	yes	yes
SRBMIP-GF	Imprinted	Substrate, coated	5 mm	GF	PBS	FLU	none	no <sup>[c]</sup>	no
NIP-GF	Imprinted	Substrate, coated	5 mm	GF	PBS	FLU	none	no <sup>[c]</sup>	no

[a] GF = glass fibre, NC = nitrocellulose; [b] retention and capture primarily because of stopped flow; [c] only when passing by this zone during flow.

the polyelectrolyte line not able to capture the dye for more than a few minutes. Such a behaviour is undesirable not only for a robust, time-independent signal readout, but long-term stability is also important for documentation purposes. Also, the application of higher concentrations does not improve the performance in a desired way because a higher PDDAC concentration only leads to a complete stop of the flow instead of selective dye capture. Employing polyelectrolytes as capture material thus seems to be less ideal as not only does the amount of potentially releasable reporter govern the amount of polyelectrolyte that has to be applied, but also does the ionic strength of the sample medium have a decisive effect. Such capture zones might therefore be used with non-buffered flowing agents and samples of low ionic background.

**Functionalized mesoporous silicas as capture matrix.** As a potential alternative to ionic polymers, mesoporous silica materials functionalized with ionic groups were considered next. Such materials have the advantage of high surface areas, which would allow for the anchoring of a large number of functional groups, and nano- to micrometric particle sizes, which guarantees that they do not move with the flow, as has been shown in many studies when these materials are used as scaffolds for gAID systems in LFAs.<sup>[9,11, 14, 19]</sup> In addition, one of the first successful applications of mesoporous silica materials was their use as capture materials in chemical remediation, and many examples ranging from metal ions to organic pollutants, including small charged organic molecules as well as dyes, have been realized until today.<sup>[20]</sup> Here, MCM-41 and SBA-15 type mesoporous materials were coated with amino groups on their inner and outer surface by way of APTES condensation, resulting in the capture materials **APTES-MCM** and **APTES-SBA** (see Experimental section and Sections 2 and 3, Supporting Information for more details about synthesis and characterisation). At buffered pH of ca. 7, at which immunochemical LFAs are commonly conducted, a large number of the amino groups is present in their protonated state which is why 2,7-dichlorofluorescein (FLU) was used as an anionic reporter dye in these experiments, guaranteeing efficient electrostatic capture. As is shown in Figure S9, nitrocellulose strips with hydrophobic wax patterns were used as LFA supports. The results obtained from these studies are also reported in Table 1, revealing that capture is much better in the MCM-41 than in the SBA-15 scaffold (Figures S9b vs S9c). When considering the similar degrees of amino group functionalization per mass of material, see Table S2, the different behaviour does not seem to be related to different functionalization degrees but more to the individual flow characteristics in the smaller pores of MCM-41 (ca. 2.5 nm diameter) compared with the larger pores of SBA-15 (ca. 8 nm diameter), the narrower pores presumably facilitating interaction of a larger number of anionic dye molecules with surface-bound ammonium groups. In addition, nanoparticles such as the MCM-41 materials can be more densely packed in the fibrous network than the SBA-15 microparticles which might reduce empty interparticle spaces through which the dye can unhinderedly diffuse. Control experiments conducted with the carboxylic acid-functionalized MCM-41 material **COOH-MCM**, for which the amino groups of

**APTES-MCM** have been almost quantitatively converted into net negatively charged carboxylate groups (Table S2), revealed that capture is essentially due to electrostatic attraction, **COOH-MCM** not retaining FLU (Figure S9d).

Up to now, the capture efficiency for anionic dyes was investigated, but in terms of an expansion of the assay toolbox, especially highly fluorescent and orange-to-red emitting cationic dyes such as many rhodamines are very interesting. To avoid retention of the reporter on nitrocellulose membranes when using such positively charged dyes, nitrocellulose commonly being net negatively charged at pH 7–8,<sup>[21]</sup> a glass fibre (GF) membrane was employed as substrate, guaranteeing unhindered flow. The respective entries in Table 1 and the results in Figure S10 show that indeed charge complementarity governs the retention efficiency of **COOH-MCM** and **APTES-MCM**, the former capturing the cationic dyes Rh6G and Rh101 while the latter solely retains anionic FLU and SRB.

In a next set of experiments, the possibility of using two materials on one strip was investigated by creating two lines of **COOH-MCM** and **APTES-MCM** in the capture zone area, to separate an anionic from a cationic dye. Two different mixtures of dyes (1  $\mu$ L, 10 ppm) were spotted on the interaction zone 2, i.e., two green-fluorescent dyes Rh6G (positively charged) and FLU (negatively charged) as well as a green- (FLU; negatively charged) and an orange-fluorescent dye (Rh101; positively charged). Whereas **COOH-MCM** was spotted in a line at ca. 3 cm from one end of the strip (L1), **APTES-MCM** was spotted at ca. 2 cm from the other end of the strip (L2). A sample and an absorbent pad were also introduced at the beginning and at the end of the strips, before introduction of the strips into a lateral flow cassette. After the development with 120  $\mu$ L of PBS, two different greenish lines or a green and an orange line were observed, associated to the retention of the respective dyes FLU (captured in L2) and Rh6G or Rh101 (concentrated in L1, Figure 2a). Again, clear separation of the dyes through retention via electrostatic forces was verified by recording the fluorescence spectra of the lines L1 and L2 (Figure 2b).

**Small molecule-functionalized cellulose and glass fibre membranes as capture matrix.** So far, the capture materials were deposited as solutions or suspensions on the test strips in the shape of lines, inherently associated with the problem of having to achieve homogeneous distribution in the fibre network simply by capillary diffusion of the deposited liquid. As a possible alternative, the chemical modification of the paper as such was considered, using small organic molecules instead of polymers or nanoparticles. In analogy to **APTES-MCM** and **COOH-MCM**, small pieces of cellulose (C) as well as glass fibre (GF) papers were coated with protonatable APTES groups, leading to **APTES-C** and **APTES-GF**. For control purposes, a part of **APTES-GF** was converted into anionic **COOH-GF**; anionic FLU was used as the model reporter. As can be seen in Table 1 and Figure S11, the retention behaviour is qualitatively similar as in the case of the mesoporous silica materials, i.e., FLU is retained in **APTES-C** and **APTES-GF** but not in **COOH-GF**. However, compared with deposited suspensions of functionalized MCM-41 particles, the performance of the papers is worse.

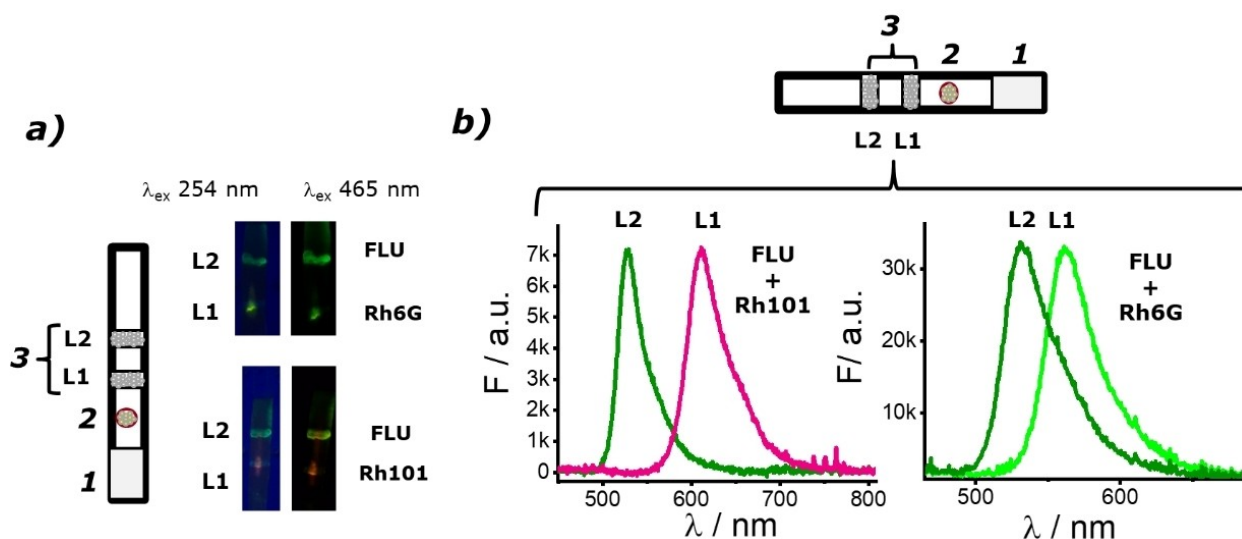


**Figure 2.** a) Photographs of zone 3 of strips under UV ( $\lambda_{\text{exc}}$  254 nm) or violet light ( $\lambda_{\text{exc}}$  465 nm) excitation containing a line of COOH-MCM as L1 and APTES-MCM as L2 in capture zone 3 after introduction of 120  $\mu\text{L}$  of PBS (80 mM) in zone 1 and flow via zone 2, in which either a mixture of Rh6G and FLU (10  $\text{mg mL}^{-1}$ ; top) or Rh101 and FLU (10  $\text{mg mL}^{-1}$ ; bottom) was deposited. b) Corresponding fluorescence emission spectra of the dyes retained in the COOH-MCM and APTES-MCM lines recorded with an optical fibre connected to a portable spectrometer.

**Imprinted polymer-functionalized glass fibre membranes as capture matrix.** The capture matrices introduced so far involve the employment of electrostatic forces to retain a charged reporter molecule in the capture zone. Despite of the efficiency of retention, however, these zones only show charge-specific capture, limiting their use in applications in which multiplexing of more than two analytes is desired. To achieve a higher flexibility here while maintaining selectivity, other recognition features have to be invoked, guaranteeing a better supramolecular selectivity through non-covalent interactions. However, binding a reporter molecule through multiple non-covalent interactions is not a very realistic approach when one has to synthesize and use a secondary receptor supramolecule for the capture of a reporter molecule in a stoichiometric fashion, because the effort and costs would be too high. A viable alternative in this respect is molecular imprinting, in which a target molecule, here the reporter, is imprinted into a network during the polymerization of adequate functional (co)monomers and crosslinkers that can interact with the target molecule by forming a multi-partner complex.<sup>[22]</sup> Such molecularly imprinted polymers (MIPs) are well-established materials for compound separation and enrichment,<sup>[23]</sup> thus constituting a promising approach for our present purpose. Based on our experience with the coating of thin MIP layers onto slides and particles<sup>[24]</sup> and in analogy to the coating of cellulose fibres,<sup>[25]</sup> we reasoned that the coating of glass-fibre membranes with MIP gels for the specific recognition of reporters might principally open the way to a true several-reporter capture in detection zones on strip that would complement well the use of modular gAID systems for multiplexed analysis as introduced recently by us.<sup>[11]</sup>

Synthetically, the gel-coated strips were prepared by immersing 5 × 5 mm pieces of a GF paper, previously functionalized with 3-(trimethoxysilyl)propyl methacrylate to equip the

support with polymerizable groups for covalently anchoring the MIP, in a prepolymerization solution containing acrylamide (AAm) and *N*-isopropylacrylamide (NIPAAm) as functional monomers, *N,N'*-ethylene bis(acrylamide) (EBAAm) as the crosslinker and either FLU or SRB as the reporter templates, before initiating polymerization (see Experimental section and Sections 2 and 4, Supporting Information for more details about synthesis and characterisation). The different amide monomers and crosslinkers were chosen because they contain charge-neutral hydrogen bond donating and accepting moieties of different strength and steric availability, yet of no pronounced acidity or basicity, potentially interacting with all the functional groups of fluoresceins and rhodamines, i.e., hydroxy, keto, carboxylic acid, sulfonic acid, secondary and tertiary amino groups while also introducing a certain hydrophobicity into the network.

To test the general approach, the efficiency of a strip coated with a fluorescein-templated MIP, **FLUMIP-GF**, was compared to that of a strip coated with a non-imprinted gel, **NIP-GF**. Such non-imprinted polymers (NIP) are synthesized in the same way as the MIPs yet in the absence of a template and exemplify important reference matrices to assess the degree of non-specific binding of such a recognition element. The corresponding entries in Table 1 and the representative results shown in Figure S12 reveal that, once the flow has had enough time to transport the cargo along the entire strip, i.e., after >4 min, the retention of FLU is only effective in **FLUMIP-GF**. The amount of dye captured in both control experiments is significantly less, i.e., the amount of the imprinted dye FLU retained in **NIP-GF** as well as the amount of a second dye as potential competitor, SRB, by **FLUMIP-GF**. Selectivity of the imprinted capture zones is essential when aiming at discrimination and multiplexing.

To demonstrate multiplexing on a single strip with MIP-type capture zones, strips containing a first zone with SRB-imprinted **SRBMIP-GF** and a second zone with **FLUMIP-GF** were prepared, and their ability for selective retention of the imprinted dye from a mixture of both dyes at 10 ppm was assessed. Figure S13 shows that SRB was only retained in the **SRBMIP-GF** zone, whereas FLU was retained only in the **FLUMIP-GF** zone. Moreover, in a control experiment with PBS containing no dye, only minor changes of the background were observed for **FLUMIP-GF** and **SRBMIP-GF**, which is ascribed to the transition of the gel from the dry to the wet state. These results suggest that the principle of using MIP gel-coated pads as capture zones is a promising one.

**Combining capture matrices and gated sensing materials on strip for gAID assays.** Having a range of different capture matrices available, the combination of antibody-gated indicator release systems with the capture matrices was approached. For that purpose, several materials for the detection of the explosives pentaerythritol tetranitrate (PETN) and 2,4,6-trinitrotoluene (TNT) were employed (see Experimental and Sections 2 and 3, Supporting Information for more details on synthesis and characterisation). In short, **gAID-1** was loaded with SRB and **gAID-2** was loaded with FLU, both of them were equipped with the gating chemistry for PETN, while **gAID-3** was loaded with tris(bipyridine)ruthenium(II) chloride (RTB) and equipped with the gating chemistry for TNT. RTB is a positively charged dye that is also expected to be better retained by net negatively charged capture materials.

In a first experiment, different strips with the simplest example of a capture matrix were prepared, i.e., with PDDAC solutions of 35%. Based on the results discussed above, strips with lines of 6 mm of a 35% PDDAC solution as capture zones were prepared. Then, 5  $\mu\text{L}$  of a 1  $\text{mg mL}^{-1}$  suspension of **gAID-1** was deposited in the interaction zone 2. A sample and an absorbent pad were introduced at the beginning and at the end of the strips, and the strips were finally introduced inside of a lateral flow cassette before development by flowing 160  $\mu\text{L}$  PBS (80 mM, containing 2.5% MeOH) spiked with either 25 ppm pentaerythritol tetranitrate (PETN) or containing no analyte in LFA fashion. Figure 3 shows that only in the presence of PETN, a considerable amount of SRB could be detected in the capture zone (Line 1).

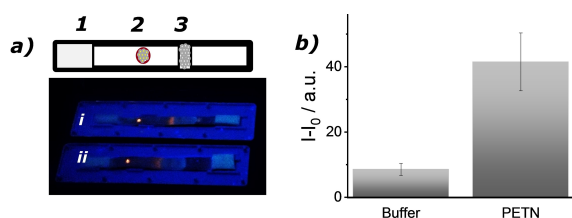


**Figure 3.** a) Test strip adapted for a lateral flow assay containing a PDDAC line (35%, 6 mm) as capture zone 3 and sensory material **gAID-1** in the interaction zone 2, after development in the presence (i) and the absence (ii) of PETN (25 ppm) in PBS 80 mM containing 2.5% MeOH as solvent spotted onto zone 1. b) Corresponding integrated fluorescence of the area of the capture zone 3 evaluated using ImageJ.

In a second experiment, the efficiency of several capture zones was evaluated. For that purpose, glass fibre paper coated with a PEG silane was used as a membrane (**PEG-GF**). The PEG coating of GF paper reduces direct ionic interactions of the capping antibodies with the matrix material thereby reducing blank release and enhancing the stability of the **gAID** ensembles.<sup>[9]</sup> 5  $\mu\text{L}$  of a 1  $\text{mg mL}^{-1}$  suspension of the **gAID-2** sensing material loaded with FLU were deposited in the interaction zone 2, and different materials were selected to be incorporated in the capture zone 3: (i) a line of PDDAC solution of 35% and (ii) a line containing **APTES-MCM**. The strips were dipped for 2 min in 100  $\mu\text{L}$  of PBS (80 mM, containing 2.5% MeOH) containing different amounts of PETN. As can be seen in Figure 4, the release of dye increased as a function of the PETN concentration. However, whereas the dye was non-homogeneously and non-symmetrically spread across the upper part of the strips when no capture matrix was incorporated, covering ca. 1  $\text{cm}^2$  of the strip, the released reporter was much more focussed when a capture material was employed, to ca. 0.25  $\text{cm}^2$  in the case of a line of PDDAC and to ca. 0.15  $\text{cm}^2$  in the case of **APTES-MCM**. In addition, the experimental error of the assay was significantly reduced. When fitting the dose–response curves to a four-parametric logistic function, limits of detection (LODs) of  $2.9 \pm 0.5$ ,  $0.9 \pm 0.2$  and  $9.2 \pm 4.3 \mu\text{g L}^{-1}$  were derived for the strips containing a PDDAC line, an **APTES-MCM** line and no line, respectively. The highest value for the blank strip is ascribed to the dye being distributed over the upper half of the strip, so that a significant number of dyes escapes detection by the LED excitation/smartphone camera system. The area-normalised intensities shown in Figure 4d underline this interpretation with the values found for the plain strips being significantly lower than in the other two cases. The somewhat lower LOD combined with a higher brightness of the **APTES-MCM** line compared with the PDDAC line also reflects well the superiority of the functionalized nanomaterial compared with the polyelectrolyte. These data are supported by the measurement uncertainties as given above, derived in analogy to our previous works,<sup>[9,11]</sup> decreasing on the order of no line > PDDAC line > **APTES-MCM** line.

**Combining capture matrices and gated sensing materials for dual-plexing on strip.** Based on the encouraging results obtained with a single **gAID** system and having in mind the unique modularity, high sensitivity and selectivity of such **gAID** systems, a dual-plexing assay for the detection of two small-molecule explosives PETN and TNT was performed by combining **gAID-2** and **gAID-3** sensing materials. To obtain a better strip reproducibility, pieces of ca. 10  $\times$  4 cm of GF paper were cut and the zones were prepared in a 4  $\times$  0.5 cm raster by depositing a suspension with a mixture of the sensor materials **gAID-2** and **gAID-3** (2  $\text{mg mL}^{-1}$  in PBS 80 mM, pH 7.5) in a thin line at a distance of ca. 5 mm from the bottom of each small strip with a lateral flow reagent dispenser, adding a second line located at a distance of ca. 1.5 cm from the bottom of the strip (containing capture material **COOH-MCM**, 10  $\text{mg mL}^{-1}$ , Milli-Q water) and a third line located at a distance of ca. 2.5 cm from the bottom of the strip (containing **APTES-MCM**, 10  $\text{mg mL}^{-1}$ , Milli-Q water). The mixture of the sensor materials **gAID-2** and

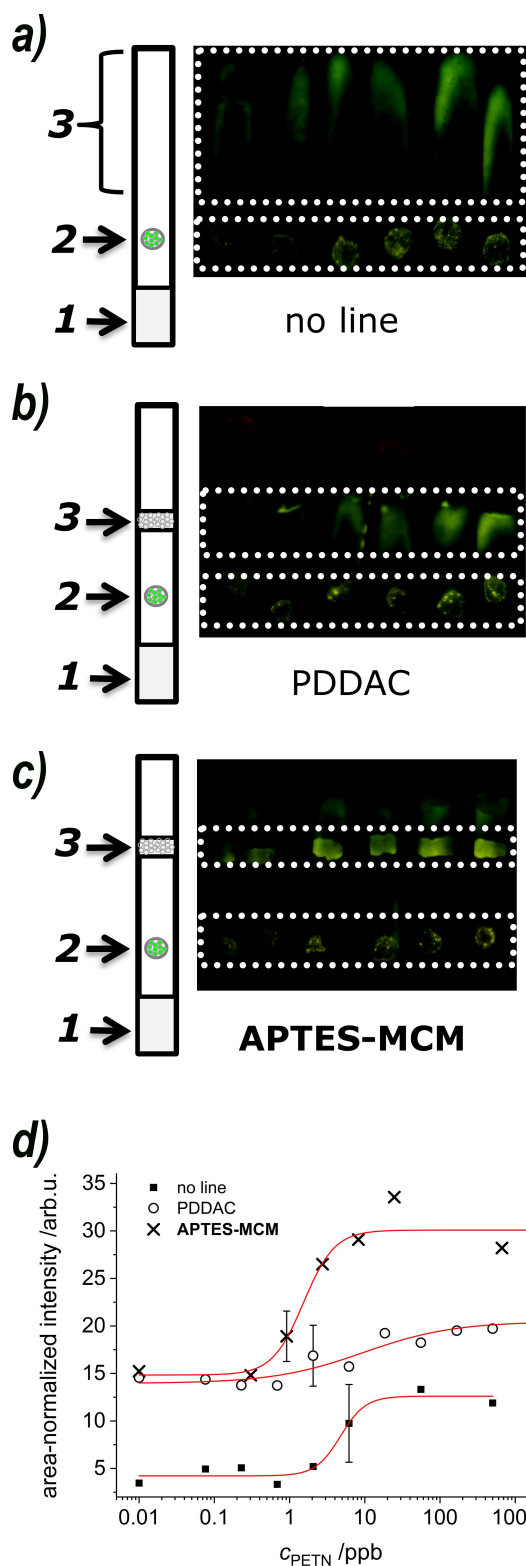


**Figure 4.** Dye released as a function of the PETN concentration on the strips containing a) no additional material, b) a PDDAC line and c) APTES-MCM in the capture zone 3; photographs of the strips show the interaction zone 2 and the capture zone 3 before flow and after flow as a function of the PETN concentration (from left to right: 0–25 ppb) under excitation with a home-made lamp. The areas encircled with a white dotted line correspond to zone 2 (bottom) and those areas in which zone 3 is located and which were analysed. d) Plot of the data extracted from the corresponding titrations.

gAID-3, COOH-MCM and APTES-MCM suspensions were applied with a dispenser, fed by a syringe pump (flow of  $0.3 \text{ mL min}^{-1}$ ), at a speed of  $5 \text{ cm s}^{-1}$ , remarking the line 3-times. Afterwards, the paper was dried for 1 h at room temperature in a vacuum and cut into the  $4 \times 0.5 \text{ cm}$  pieces used for the assays.

Following a similar procedure as described above, the strips were dipped into 100  $\mu\text{L}$  of PBS (80 mM, containing 2.5% MeOH, pH 7.5) for 2 min containing different amounts of PETN, TNT or a mixture of these two explosives. As can be seen in Figure 5, when only TNT was present in the solution, the intensity of the orange fluorescence in L1 increased as a function of the TNT concentration due to the release of positively charged RTB from gAID-3 whereas the intensity of L2 remained constant and increased only moderately with higher amounts of TNT. The initial background signal in the absence of TNT is due to a certain blank release of the sensory material and background fluorescence. When the experiment was repeated in the presence of PETN, an increased green

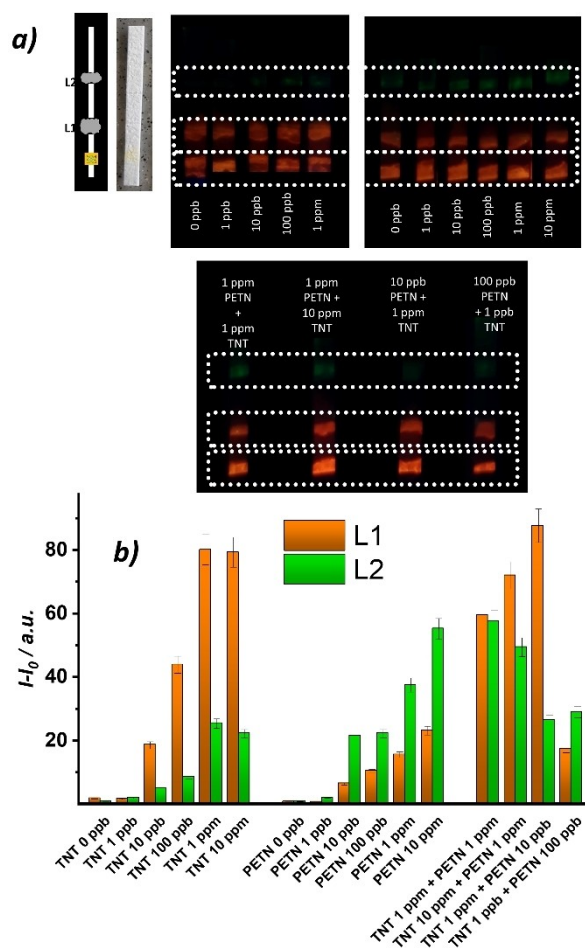


**Figure 5.** a) Photographs of strips showing the interaction zone 2 (containing a mixture of gAID-2 and gAID-3 sensing materials) and capture zone lines L1 (COOH-MCM) and L2 (APTES-MCM) before flow and after flow as a function of the PETN or TNT concentration as well as in presence of both explosives at different concentration ratios under excitation with a home-made lamp. b) Corresponding intensity of fluorescence registered in L1 and L2.

fluorescence was observed in L2 as a function of the concentration of PETN, because of release of fluorescein from **gAID-2**, the resulting background signal in L1 being caused as described before. To assess the separation ability of the approach, both explosives were used in mixtures at different concentrations, showing an encouraging dual-plexing performance.

In a last series of experiments, the performance of the strips in the presence of three different real-world sample matrices was tested, sea water, wine, and milk, evaluating how the ensemble of **gAID-2** and **gAID-3** materials in combination with **APTES-MCM** and **COOH-MCM** accomplishes analyte detection in a more realistic scenario. The test strips were thus dipped into mixtures of 100  $\mu\text{L}$  PBS and the liquid samples at a ratio of 75:25 for 2 min, containing a final concentration of 1 ppm of PETN and TNT. Diluting the samples with buffer is necessary to guarantee full function of the immunochemical gating chemistry, closing the pores of the **gAID** systems.<sup>[11,16]</sup> As can be seen in Figure S14, the performance was virtually identical in the three real sample matrices, the fluorescence responses being only somewhat different to the fluorescence in neat buffer. Detrimental matrix effects were thus not observed, suggesting that the systems using functionalized MCM particles in the capture zone is rather sample-tolerant.

## Conclusion

In the present contribution, the use of certain macromolecules or materials immobilized in the detection zone of test strips has been reported with the aim to create label-free and potentially multiplexed detection zones for lateral flow assays, in particular for LFAs that operate via gated indicator release. For this purpose, polyelectrolytes, mesoporous materials, chemically modified cellulose or glass fibre membranes and molecularly imprinted polymer gels coated onto membranes were conceived and tested as potential candidates for the capture of various indicator dyes that act as reporters in antibody-gated indicator delivery (**gAID**) assays. Whereas the polyelectrolyte materials showed a rather inferior performance, being susceptible to buffers/electrolytes that are commonly present in a sample/assay solution, functionalized mesoporous silicas and MIPs revealed promising behaviour. After having identified the best material of this study in model assays, combination with a **gAID** sensing material responding to PETN allowed to assess the improvement of this capture zone approach compared to the conventionally used blank strips, showing a distinct improvement of the analysed images in terms of limit of detection and measurement uncertainty. As a second key feature of the present work, it could be shown that this capture zone approach together with **gAID** materials is a promising way to approach low number multiplexing on test strips for use in very simple settings, as demonstrated with the dual-plexing detection of TNT and PETN. In view of the other low-number multiplexing approach that we have recently introduced, a multi-channel strip instead of a single-channel strip (see beginning of Results and Discussion section), the multi-channel

strip has the drawbacks that the analyte is divided by the number of channels, that homogeneous and parallel flow is more difficult to achieve and that homogeneous irradiation in a smartphone case of simple architecture is also difficult to achieve with a single LED. However, apart from the question of single- vs. multi-channel architecture, it is especially their combination which should be kept in mind. Realistically, the number of analytes to be detected on a single strip will not exceed three or four, so that combination of such strips in a three-channel setup might already allow to go for nine or twelve analytes, which is a number of lead analytes that would be very helpful in typical on-site rapid testing scenarios. The findings reported here also highlight the modularity and tunability of the system, allowing facile adaption to a specific assay under consideration. Equipping tailored tests strips with capture zones for reporter focussing will stimulate research and development into the direction of ASSURED tests, i.e., tests that are affordable, sensitive, specific, user-friendly, rapid and robust, equipment free and deliverable to end-users,<sup>[26]</sup> for key or lead parameter detection in the medical diagnostic, environmental, security and food sectors, facilitating the implementation of label-free detection and inherent signal amplification.

## Experimental Section

**Synthesis of MCM-41 and SBA-15 type mesoporous materials.** The syntheses of the MCM-41 and the SBA-15 type mesoporous materials were performed following previously reported procedures; details can be found in Section 2.1 and 2.2, Supporting Information.<sup>[27]</sup>

**Functionalisation of materials with amino and carboxylic acid groups.** The mesoporous silica materials were modified in one or two steps with 3-aminopropyltriethoxysilane (APTES) or APTES and succinic anhydride, yielding **APTES-MCM** and **APTES-SBA** or **COOH-MCM**, according to reported procedures; details can be found in Sections 2.3 and 2.4, Supporting Information.<sup>[27,28]</sup>

**Synthesis of gated hybrid materials.** In this work, three antibody-gated materials for the detection of PETN (**gAID-1** and **gAID-2**) and TNT (**gAID-3**) were employed as examples for gated indicator release systems to be used in zone 2 of the lateral flow approach introduced above and to perform dual-plexing experiments. The preparation of these gated materials and their precursors **SRB@MCM**, **FLU@MCM** and **RTB@MCM** was carried out in analogy to our earlier works;<sup>[11,29]</sup> and the details of the syntheses can be found in Sections 2.5–2.9, Supporting Information.

**Synthesis of APTES-functionalized cellulose (APTES-C) and glass fibre papers (APTES-GF).** For modification of cellulose and glass fibre paper with amino groups, 20 pieces of the corresponding paper (2  $\times$  0.5 cm) were suspended in 7 mL of toluene and 100  $\mu\text{L}$  of APTES. The samples were stirred for 16 h at 80  $^{\circ}\text{C}$ . The resulting amino-modified papers were collected and then washed twice with toluene and once with EtOH, before drying in a vacuum for 3 h, yielding the papers **APTES-C** and **APTES-GF**. The strips were cut into smaller pieces of 0.5  $\times$  0.5 cm for integration with the LFA strips.

**Synthesis of COOH-functionalized cellulose (COOH-C) and glass fibre papers (COOH-GF).** For the modification of **APTES-C** and **APTES-GF** papers with carboxylic acid groups, five pieces of each paper were mixed with 1.5 mL of EtOH, following reported



procedures.<sup>[28]</sup> 250  $\mu\text{L}$  of a solution of succinic anhydride (100  $\text{mg mL}^{-1}$ ) were added to each of the mixtures prepared, and were left to stir overnight at 40 °C. Then, the papers were removed and washed twice with 1.5 mL of EtOH. Finally, the papers were dried in a vacuum at 40 °C for 2 h, yielding the papers COOH-C and COOH-GF. The strips were cut into smaller pieces as above.

**Synthesis of methacrylate-functionalized glass fibre paper (M-GF).** Glass fibre paper was modified with methacrylate groups following the same procedure described for APTES-GF but using 3-(trimethoxysilyl)propyl methacrylate instead of APTES, yielding M-GF.

**Synthesis of PEG-coated glass fibre paper (PEG-GF).** A mixture of 3.4 mL Milli-Q  $\text{H}_2\text{O}$ , 7.4 mL EtOH, 2.7 mL tetraethylorthosilicate (TEOS), 300  $\mu\text{L}$  of 2-(methoxy(polyethyleneoxy)propyl)trimethoxysilane (PEG silane) and 180  $\mu\text{L}$   $\text{NH}_3$  (32%) was added into a vial of 20 mL containing 30 glass fibre strips of 4  $\times$  0.5 cm. The reaction was left to proceed for 24 h at room temperature with orbital stirring. The final coated paper was washed with EtOH and dried under reduced pressure, yielding PEG-GF.

**Synthesis of glass fibre papers coated with imprinted polymer gels (FLUMIP-GF and SRBMIP-GF).** Glass fibre papers coated with molecularly imprinted polymer (MIP) gels were prepared using an aqueous precipitation polymerization method following literature procedures.<sup>[30]</sup> Typically, 10 pieces of M-GF (2  $\times$  0.5 cm) were mixed with 6 mL of a PBS solution (20 mM; pH 7.2) containing acrylamide (AAm; 29.1 mg, 0.41 mmol) and *N*-isopropylacrylamide (NIPAAm; 46.4 mg, 0.41 mmol). 150  $\mu\text{L}$  of a solution of 5 mM of the corresponding template molecule 2,7-dichlorofluorescein (FLU) or sulforhodamine B (SRB) were added to the solution, and the mixture was incubated for 30 min with slow stirring at 25 °C to form complexes. After that, the cross-linker *N,N'*-ethylene bis(acrylamide) (EBAAm; 25.2 mg; 0.15 mmol) was added. After purging the mixture with  $\text{N}_2$  for 1 h, polymerization was initiated by adding ammonium persulfate (APS; 6 mg) and *N,N,N',N'*-tetramethylethylenediamine (TEMED; 3  $\mu\text{L}$ ). The reaction was continued for 1 h at 25 °C under a  $\text{N}_2$  atmosphere, observing the formation of the gel after 10 min. After 1 h of reaction, the resulting MIP gel-coated papers were collected by removing them from the gel, followed by extensive washing with NaCl solution (1 M) until complete removal of the unreacted monomers and templates. Whereas removal of FLU was virtually quantitative, a residual pink colour remained on the SRBMIP-GF strips, suggesting that a certain fraction of the SRB molecules is locked in cavities and cannot be removed even by extensive washing. Finally, the corresponding papers were dried for 2 h in a vacuum, yielding FLUMIP-GF and SRBMIP-GF. For control purposes, non-imprinted gels on paper (NIP-GF) were also prepared in the same way except that no template was added during polymerization. The strips were cut as above.

**Characterisation of materials.** The presence of the materials' mesoporous structure of both MCM-41 and SBA-15 type materials was confirmed with transmission electron microscopy (TEM) analysis and nitrogen adsorption-desorption isotherms, whereas the respective contents of organic substance on and in the materials were determined by elemental analysis, thermogravimetry and spectrophotometric measurements (see Section 3, Supporting Information including Figures S1, S2 and Tables S1–S3).

**Characterisation of functionalised papers.** The different modified papers were first analysed under an optical microscope and in more detail with a Scanning Electron Microscope (SEM), see Figures S3, S4, Supporting Information), whereas the different degrees and types of functionalisation of the membranes were examined quantitatively with TGA. In addition, FTIR spectroscopy

and SEM with energy dispersive X-ray microanalysis (SEM-EDX) were employed to qualitatively confirm the different functional groups on the paper (see Section 5, Supporting Information including Figures S3–S6 and Tables S4, S5).

## Acknowledgements

Financial support from Germany's Federal Ministry for Economic Affairs and Energy and the German Research Foundation (DFG; CL 761/1-19) is gratefully acknowledged. We thank S. Ast for fruitful discussions, S. Selve (Technical University Berlin) and Kornelia Gawlitza (BAM, Chem. Opt. Sens. Div.) for TEM images, A. Zehl (Humboldt University Berlin) for elemental analysis, M. Grüneberg (BAM, Chem. Opt. Sens. Div.) for thermogravimetric analysis, A. Zimathies (BAM, Struct. Anal. Div.) for  $\text{N}_2$  adsorption/desorption measurements, S. Benemann (BAM, Surf. Anal. Interfacial Chem. Div.) and C. Tobias (BAM, Chem. Opt. Sens. Div.) for SEM and EDX measurements, A. Kohl (BAM, Process Anal. Technol. Div.) for FTIR measurements, R. Gotor and J. Bell (BAM, Chem. Opt. Sens. Div.) for the assembly of the home-made fluorescence lamp and J. Bell for help with the measurements of real-life samples. Open access funding enabled and organized by Projekt DEAL.

## Conflict of Interest

The authors declare no conflict of interest.

## Data Availability Statement

The data that support the findings of this study are available from the corresponding author upon reasonable request.

**Keywords:** gated delivery · mesoporous materials · molecularly imprinted polymers · rapid tests · test strips

- [1] a) K. Luo, H. Y. Kim, M. H. Oh, Y. R. Kim, *Crit. Rev. Food Sci. Nutr.* **2020**, *60*, 157–170; b) N. Jiang, R. Ahmed, M. Damayantharan, B. Unal, H. Butt, A. K. Yetisen, *Adv. Healthcare Mater.* **2019**, *8*, 1900244; c) C. Dincer, R. Bruch, E. Costa-Rama, M. T. Fernandez-Abedu, A. Merkoci, A. Manz, G. A. Urban, F. Guder, *Adv. Mater.* **2019**, *31*, 1806739; d) H. Manisha, P. D. Priya Shwetha, K. S. Prasad, in *Environmental, Chemical and Medical Sensors* (Eds.: S. Bhattacharya, A. K. Agarwal, N. Chanda, A. Pandey, A. K. Sen), Springer, Singapore, **2018**, pp. 315–341.
- [2] R. Antiochia, *Biosensors* **2021**, *11*, 110.
- [3] a) M. Sajid, A.-N. Kawde, M. Daud, *J. Saudi Chem. Soc.* **2015**, *19*, 689–705; b) F. Di Nardo, M. Chiarello, S. Cavalera, C. Baggiani, L. Anfossi, *Sensors* **2021**, *21*, 5185.
- [4] C. Parolo, A. Sena-Torrallba, J. F. Bergua, E. Calucho, C. Fuentes-Chust, L. M. Hu, L. Rivas, R. Alvarez-Diduk, E. P. Nguyen, S. Cinti, D. Quesada-Gonzalez, A. Merkoci, *Nat. Protoc.* **2020**, *15*, 3788–3816.
- [5] a) G. Y. Zhu, X. D. Yin, D. L. Jin, B. Zhang, Y. Y. Gu, Y. R. An, *TrAC Trends Anal. Chem.* **2019**, *111*, 100–117; b) L. Huang, S. L. Tian, W. H. Zhao, K. Liu, X. Ma, J. H. Guo, *Analyst* **2020**, *145*, 2828–2840.
- [6] a) M. Jauset-Rubio, M. S. El-Shahawi, A. S. Bashammakh, A. O. Alyoubi, C. K. O'Sullivan, *TrAC Trends Anal. Chem.* **2017**, *97*, 385–398; b) R. Reid, B. Chatterjee, S. J. Das, S. Ghosh, T. K. Sharma, *Anal. Biochem.* **2020**, *593*, 113574.

- [7] a) L. Anfossi, F. Di Nardo, S. Cavalera, C. Giovannoli, C. Baggiani, *Biosensors* **2018**, *9*, 2; b) N. A. Taranova, N. A. Byzova, V. V. Zaiko, T. A. Starovoitova, Y. Y. Vengerov, A. V. Zherdev, B. B. Dzantiev, *Microchim. Acta* **2013**, *180*, 1165–1172; c) P. L. A. M. Corstjens, K. Kardos, R. S. Niedbala, H. J. Tanke, M. Zuiderwijk, H. H. Feindt, V. K. Mokkapatil, J. A. Kimball (Orasure Technologies, Inc.), US20070105237 A1, **2007**; d) I. Mendel-Hartvig, R. Bjoerkman, G. Rundstroem (Pharmacia Diagnostics AB), WO2003025573 A1, **2003**.
- [8] M. Hecht, E. Climent, M. Biyikal, F. Sancenón, R. Martínez-Máñez, K. Rurack, *Coord. Chem. Rev.* **2013**, *257*, 2589–2606.
- [9] E. Costa, E. Climent, S. Ast, M. G. Weller, J. Canning, K. Rurack, *Analyst* **2020**, *145*, 3490–3494.
- [10] J. Lei, H. Ju, *Chem. Soc. Rev.* **2012**, *41*, 2122–2134.
- [11] E. Climent, M. Biyikal, D. Gröninger, M. G. Weller, R. Martínez-Máñez, K. Rurack, *Angew. Chem. Int. Ed.* **2020**, *59*, 23862–23869; *Angew. Chem.* **2020**, *132*, 24071–24078.
- [12] E. Climent, K. Rurack, *Angew. Chem. Int. Ed.* **2021**, *60*, 26287–26297.
- [13] S. Kasetsirikul, M. J. A. Shiddiky, N. T. Nguyen, *Microfluid. Nanofluid.* **2020**, *24*, 17.
- [14] E. Costa, E. Climent, K. Gawlitza, W. Wan, M. G. Weller, K. Rurack, *J. Mater. Chem. B* **2020**, *8*, 4950–4961.
- [15] E. Climent, M. Hecht, K. Rurack, *Micromachines* **2021**, *12*, 249.
- [16] E. Climent, M. G. Weller, R. Martínez-Máñez, K. Rurack, *ACS Appl. Nano Mater.* **2022**, *5*, 626–641.
- [17] V. C. Özalp, D. Çam, F. J. Hernandez, L. I. Hernandez, T. Schäfer, H. A. Öktem, *Analyst* **2016**, *141*, 2595–2599.
- [18] Y. Zhao, H. R. Wang, P. P. Zhang, C. Y. Sun, X. C. Wang, X. R. Wang, R. F. Yang, C. B. Wang, L. Zhou, *Sci. Rep.* **2016**, *6*, 21342.
- [19] E. Climent, D. Gröninger, M. Hecht, M. A. Walter, R. Martínez-Máñez, M. G. Weller, F. Sancenón, P. Amorós, K. Rurack, *Chem. Eur. J.* **2013**, *19*, 4117–4122.
- [20] a) J. Liu, X. D. Feng, G. E. Fryxell, L. Q. Wang, A. Y. Kim, M. L. Gong, *Adv. Mater.* **1998**, *10*, 161–165; b) M. Barczak, R. Dobrowolski, P. Borowski, D. A. Giannakoudakis, *Microporous Mesoporous Mater.* **2020**, *299*, 110132; c) S. B. Wang, H. T. Li, *Microporous Mesoporous Mater.* **2006**, *97*, 21–26; d) P. Prarat, P. Hongsawat, P. Punyapalaku, *Environ. Sci. Pollut. Res. Int.* **2020**, *27*, 6560–6576.
- [21] a) J. M. Gershoni, G. E. Palade, *Anal. Biochem.* **1983**, *131*, 1–15; b) E. Handman, H. M. Jarvis, *J. Immunol. Methods* **1985**, *83*, 113–123.
- [22] a) *Molecularly imprinted polymers: man-made mimics of antibodies and their application in analytical chemistry*, (Ed.: B. Sellergren), Elsevier Science, Oxford, **2000**; b) M. J. Whitcombe, E. N. Vulfson, *Adv. Mater.* **2001**, *13*, 467–478.
- [23] a) W. J. Cheong, S. H. Yang, F. Ali, *J. Sep. Sci.* **2013**, *36*, 609–628; b) F. Lanza, B. Sellergren, *Chromatographia* **2001**, *53*, 599–611; c) S. Torres-Cartas, M. Catala-Icardo, S. Meseguer-Lloret, E. F. Simo-Alfonso, J. M. Herrero-Martinez, *Separations* **2020**, *7*, 69.
- [24] a) R. Wagner, W. Wan, M. Biyikal, E. Benito-Pena, M. C. Moreno-Bondi, I. Lazraq, K. Rurack, B. Sellergren, *J. Org. Chem.* **2013**, *78*, 1377–1389; b) S. Wagner, J. Bell, M. Biyikal, K. Gawlitza, K. Rurack, *Biosens. Bioelectron.* **2018**, *99*, 244–250; c) W. Wan, A. B. Descalzo, S. Shinde, H. Weisshoff, G. Orellana, B. Sellergren, K. Rurack, *Chem. Eur. J.* **2017**, *23*, 15974–15983.
- [25] W. Li, X. Zhang, T. Li, Y. Ji, R. Li, *Anal. Chim. Acta* **2021**, *1148*, 238196.
- [26] S. Smith, J. G. Korvink, D. Mager, K. Land, *RSC Adv.* **2018**, *8*, 34012–34034.
- [27] E. Climent, M. Biyikal, K. Gawlitza, T. Dropa, M. Urban, A. M. Costero, R. Martínez-Máñez, K. Rurack, *Chem. Eur. J.* **2016**, *22*, 11138–11142.
- [28] D. Sarma, K. Gawlitza, K. Rurack, *Langmuir* **2016**, *32*, 3717–3727.
- [29] A. Hesse, M. Biyikal, K. Rurack, M. G. Weller, *J. Mol. Recognit.* **2016**, *29*, 88–94.
- [30] Z. Zhang, J. Liu, *RSC Adv.* **2015**, *5*, 91018–91025.

---

Manuscript received: December 11, 2021  
Revised manuscript received: April 20, 2022  
Accepted manuscript online: April 21, 2022  
Version of record online: May 12, 2022